Journal of the Korean Crystal Growth and Crystal Technology
Vol. 19, No. 5 (2009) 215-222

Crystal growth from melt in combined heater-magnet modules

P. Rudolph†, M. Czupalla, N. Dropka, Ch. Frank-Rotsch, F.-M. Kieβling, O. Klein*, B. Lux, W. Miller, U. Rehse and O. Root

Leibniz Institute for Crystal Growth (IKZ), Max-Born-Str. 2,12489 Berlin, Germany
**Weierstrass-Institute for Applied Analysis and Stochastics (WIAS), Mohrenstraße 39,10117 Berlin, Germany*

(Received August 3, 2009)
(Revised August 26, 2009)
(Accepted September 11, 2009)

Abstract Many concepts of external magnetic field applications in crystal growth processes have been developed to control melt convection, impurity content and growing interface shape. Especially, travelling magnetic fields (TMF) are of certain advantages. However, strong shielding effects appear when the TMF coils are placed outside the growth vessel. To achieve a solution of industrial relevance within the framework of the KRIST*MAG*® project inner heater-magnet modules (HMM) for simultaneous generation of temperature and magnetic field have been developed. At the same time, as the temperature is controlled as usual, e.g. by DC, the characteristics of the magnetic field can be adjusted via frequency, phase shift of the alternating current (AC) and by changing the amplitude via the AC/DC ratio. Global modelling and dummy measurements were used to optimize and validate the HMM configuration and process parameters. GaAs and Ge single crystals with improved parameters were grown in HMM-equipped industrial liquid encapsulated Czochralski (LEC) puller and commercial vertical gradient freeze (VGF) furnace, respectively. The vapour pressure controlled Czochralski (VCz) variant without boric oxide encapsulation was used to study the movement of floating particles by the TMF-driven vortices.

Key words Melt crystal growth, Travelling magnetic field, Combined heater-magnet module

1. Introduction

Today, important melt growth methods are Czochralski (Cz) and unidirectional solidification (Bridgman or vertical gradient freeze -VGF). A wide range of crystalline materials is produced by these techniques being the basis for numerous high-tech branches, such as electronics, optics and photovoltaic. The basic principles for these growth methods are well mastered and matured in industry. Therefore, the current challenges are primarily focused on further improvement of crystal quality and reduction of production costs. The latter includes the use of increased melt masses. However, as a result of such scaling-up, convective perturbations and even turbulences appear within the melts that produce large temperature fluctuations that result in compositional micro-inhomogeneities, so called “striations” within the grown crystals. Additionally, uncontrolled melt convection may cause harmful deformations of the melt-solid interface shape. To counteract this situation the use of magnetic fields are helpful. A positive effect is also obtained by artificial magnetic mixing that reduces the occurrence of constitutional supercooling at the propagating interface. As a result, during the last decades, numerous successful crystallization experiments with metals, alloys, semiconductors, and protein crystals in different kinds of magnetic fields were carried out, e.g. [1-5].

Especially, the application of non-steady magnetic fields came to the fore due to their high interaction efficiency and well-controllable stirring ability, both at relatively low magnetic induction forces. Even by using TMF the interface morphology and impurity transport can be manipulated very favourably. Until now, TMFs have been mostly applied in vertical Bridgman or VGF arrangements [6-8]. But there are also few reports on successful experiments with TMF at Czochralski growth of silicon crystals showing lowered oxygen concentration [9-11]. So far, for liquid encapsulated Czochralski (LEC) growth of semiconductor compounds such type of magnetic field was not yet tested experimentally.

Generally, strong shielding effects appear when the conventional technique is used where the TMF coils are placed outside the growth vessels. As a result, nearly one order of magnitude higher magnetic induction must be produced than is required within the melt [12]. To achieve a solution of industrial scale within the framework of the KRIST*MAG*® project (2005~2008) inner heater-magnet modules for *simultaneous generation of*

†Corresponding author
Tel: +0049+30+63923034
Fax: +0049+30+63923003
E-mail: rudolph@ikz-berlin.de

heat and magnetic fields close to the melt containers were developed [13-17]. Striking LEC and VGF results in such HMMs are presented.

2. The Features of Travelling Magnetic Field

A TMF is generated by means of applying out-of-phase alternating currents to a number of coils arranged vertically one upon the other, or of interleaved connected spirals. As a result, a meridional travelling Lorentz field is induced when an electrocontactive melt is inside applied. The field line direction (up- or downward and out- or inward in coil or spiral mode, respectively), frequency f, phase shift φ and amplitude I can be controlled very conveniently. Even TMFs show the advantage of axisymmetric toroidal roll patterns. This manifests its effective counter-acting property against buoyancy-driven convection generating mostly toroidal vortices. Further, a higher damping efficiency is obtained due to its proportionality with the field frequency. The needed induction strength of the TMF field can be estimated by

$$B \approx \sqrt{F_B/\sigma\pi f L} \qquad (1)$$

with $F_B = \rho\beta g\Delta T$ the force density of natural buoyancy-driven convection (ρ - melt density, β - volume expansion coefficient, g - gravitational acceleration, ΔT - characteristic temperature difference, σ - electrical conductivity, f - TMF frequency, L - characteristic length, e.g crucible radius). In industrial Czochralski and LEC crucibles F_B amounts to 200 N m^{-3} and 450 N m^{-3} for Si and GaAs melts, respectively, when ΔT is assumed to be 50 K. Thus, according Eq. (1) the required value of B is in the region of only few mT when field frequencies between 50 Hz and 100 Hz are induced. The close position of HMM to the melt containers ensure large penetration (skin) depth

$$\delta_s = (\pi\mu_o\mu_r\sigma f)^{-1/2} \qquad (2)$$

where μ_o is the magnetic field constant (= 12.566×10^{-7} H m^{-1}) and $\mu_r \approx 1$ the relative permeability. Skin depths of $\delta_s \approx 20$ and 2 cm appear in a GaAs melt when TMF frequencies f = 10 Hz and 600 Hz are used, respectively.

Finally, even in VGF arrangements TMF proves to be most suitable to control the shape of the growing interface [18, 19]. However, one critical point of TMF is noteworthy. For each given crystal growth system, the field strength has to be adjusted carefully since, otherwise, undesirable oscillating instabilities might appear. The criterion is given by the TMF-related Taylor number of the melt

$$Ta_{TMF} = \frac{\sigma\pi f r^3}{\rho\nu^2 k} B^2 \qquad (3)$$

with r - crucible radius, ν - kinematic viscosity, $k = 2\pi/\lambda$ - TMF wave number and λ - wavelength. Schwesig et al. [18] found numerically that the critical Taylor number Ta_{TMF^*} is about 2×10^7 with r = 2,53 cm being nearly not depending on the aspect ratio H/D (H - height, D - diameter). We observed identical result for VGF growth of 4-inch Ge [19].

3. Design and Parameters of Heater-magnet Modules

Fig. 1a shows a HMM for coupled generation of temperature and a travelling magnetic field, suitable for incorporation into industrial Cz pullers and VGF equipments. It replaces the standard heater without additional required space. However, its design must be changed from a "picket fence" (meander) shape to a coil one

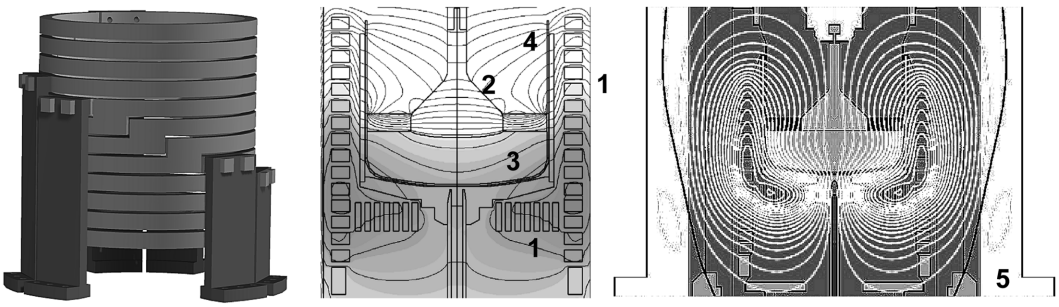

Fig. 1. a - heater-magnet module (HMM) made of graphite with staircase-shaped current path subdivided in three sections for TMF generation by feeding with three-phase current of given phase shift in star connection; b - modelled temperature field generated by the HMM (1) within the LEC puller for growth of GaAs crystals (2) from the melt (3) in a pBN crucible (4); c - snapshot of the travelling magnetic field produced within the high-pressure vessel (5) by the HMM shown in Fig. 1b.

with an upwards-winding slit forming a single layered spiral- or staircase-shaped current path (Fig. 1a). For the growth of LEC GaAs crystals a special multi-coil design was worked out [20] to generate simultaneously vertical and horizontal TMFs by jacket and bottom HMMs (pos. 1 in Fig. 1b) positioned around the wall and under the bottom of the crucible. Such arrangement proved to be the favourable one for optimal Lorentz field against buoyancy-driven temperature oscillations below the pulled crystal (Fig. 1c). Both jacket and bottom THM parameters could be varied in the travelling direction (down- or upwards in the jacket region, in- and outwards in the bottom region), frequency f and phase angle φ. The coil sections were power- and temperature-controlled in order to held the temperature field constant when various f/φ ratios were selected.

For VGF growth of Ge crystals a jacket HMM was inserted in a commercial furnace [19]. It is subdivided into three coil segments connected by star-type wiring with a power-controller system for simultaneous delivering of both DC and AC with variable amplitude, frequency and phase shift. Bottom and top heater, responsible to adjust the axial temperature gradient, were used in unmodified standard version. Special configurations of the power supplying bars were constructed in order to reduce their influence on magnetic field symmetry [16]. Fig. 2 shows the scheme of the applied VGF arrangement with HMM. The crystallization process was provided by computer-controlled gradient propagation of the DC share.

To supply the HMM with required power, frequency and phase shift a universal controller system has been developed and performed. It contains Semikron integrated intelligent power systems (SkiiP) impulse- and frequency-driven by an electronic control module. As a result both a three-phase well-formed sinus AC of desired frequency and phase shift for TMF generation and a DC component for controlling the melting and crystallization temperature are supplied to the heater-magnet. For our experiments the following parameter range was available: maximum power P = 40 kW, voltage V = 0…40 V, maximum current I = 330 A per coil section, frequency f = 10…600 Hz, phase shift φ = 5…120°. By means of such variables the generation of magnetic induction B = 1…10 mT and Lorentz force densities F_m up to about 900 N m^{-3} were possible, more than enough to counteract F_B calculable according to Eq. (1).

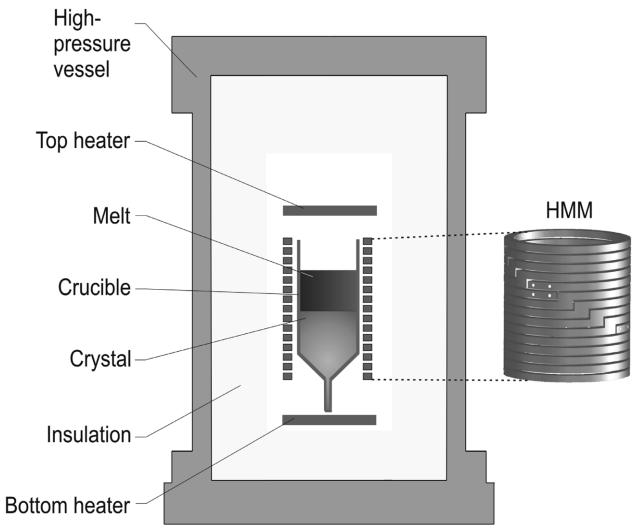

Fig. 2. Sketch of the VGF furnace with inserted HMM for the growth of Ge single crystals in travelling magnetic fields.

4. Numeric Modelling

2.5 and 3D global numeric modelling of the temperature distribution, convection patterns and growing interface shape without and with acting TMF have been carried out. The numerous results were used to optimize the single crystal growth processes, as it was published elsewhere [12, 21, 22]. It has been found that two contrarily directed THM waves, independently generated within the jacket and bottom sections of the HMM in the LEC puller (Fig. 1c), may produce a favourable Lorentz force field that separates the weak flow under the growing crystal (Taylor-Proudman cell) from the intense non-steady vortices in the crucible wall region. As a result, the temperature oscillation can be markedly dampened and shifted to less dangerous higher frequencies very effectively.

In the VGF arrangement the Lorentz force density was simulated for each coil segment in such a manner that the effective power could not exceed the power for heat generation required for the melting and crystallization process (in the range of 4~5 kW), which were obtained from the temperature field simulations and delivered by the DC share. The numerical optimization of the shape of the solid-liquid interface during the crystallization was carried out by means of snapshots of different growth positions. Additionally, the transition value of the TMF force from steady-state situation to time-dependent melt flow was studied by 3D time-dependent simulations in order to find out the uncritical TMF conditions according to Eq. (3). In Fig. 3, snapshots of the calculated time-dependent 3D temperature fields within the VGF Ge melt at aspect ratio H/D = 0.6 for uncritical

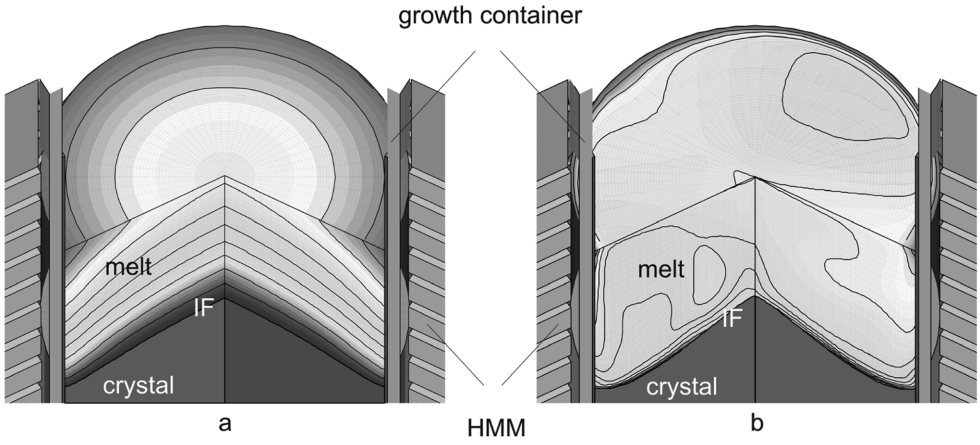

Fig. 3. 3D numerical simulation with CrysMAS code of the VGF temperature field within the Ge melt at aspect ratio H/D = 0.6. a - undercritical TMF parameters ($B \approx 2.5$ mT, $Ta_{TMF} < Ta_{TMF^*}$) ensuring nearly oscillation-free temperature field and flat solid-melt interface (IF). b - overcritical TMF conditions ($B \approx 6$ mT, $Ta_{TMF} > Ta_{TMF^*}$) leading to an inhomogeneous and markedly fluctuating temperature field.

(a) and overcritical TMF conditions (b) are compared. In order to ensure stable growth conditions with slightly convex growing interface the TMF parameters of I = 120 A/coil segment, f = 20 Hz and $\varphi = 60^o$ were found to be most suitable. The induced magnetic flux intensity of $B \approx 2.5$ mT guaranteed a laminar flow regime with uniform isotherm courses (Fig. 3a) and oscillation amplitudes (< 0.05 K), which were not quantifiable. Although the Taylor number of $Ta_{TMF} \approx (2\sim3) \times 10^7$ approached the critical one, a still stationary regime was obtained. Compared to this a markedly inhomogeneous fluctuating isotherm field was obtained (Fig. 3b) at an induction of $B \approx 6$ mT and related $Ta_{TMF} \approx 10^8$. In this case, the time analysis by Fast-Fourier-Transformation (FFT) revealed a characteristic temperature oscillation frequency of f = 0.18 Hz with an amplitude of $\Delta T \approx +/- 1$ K.

Note, the interface curvature does not keep invariable and the convexity tends to increase with decreasing H/D ratio during the whole growth process using constant TMF parameters. Considering this fact, the application of a time-depending TMF program is required that adapts each growth situation. In order to maintain a constant slightly convex interface curvature over the whole VGF process the total power must be gradually reduced from 4.5 to 4.0 kW and the TMF responsible AC share from 3.0 to 2.0 kW when a field frequency of f = 20 Hz and a phase shift of $\varphi = 60^o$ are selected [19].

5. Dummy Measurements

For the experimental validation of the numerically determined Lorentz force density, the mass responses Δm of a dummy made of stainless steel with an electrical conductivity of $\sigma = 1.3 \times 10^6$ S m^{-1} was measured when the TMF of given I, f and φ was switched on (note such value of s is nearly identically with those of Ge and GaAs melts). The dummy was a hollow cylinder with height of 35 mm and wall thickness selected according to the melt mass at real growth situation. It was hanging inside the HMM on a steel rod, which was connected with a load cell of a high-precision balance system as it is usually used for crystal weighing at Czochralski growth. The Lorentz force density was determined along the whole HMM length by moving of the dummy in 10 mm steps. The weight response $F_w = \Delta mg$ can be converted into axial Lorentz force intensity by the relation

$$F_{Lz} = \Delta mg\ V^{-1} \quad (4)$$

with g the gravitational acceleration and V the dummy volume. The measurements were carried out on air at open top of the VGF vessel. At I = 180 A, f = 500 Hz and $\varphi = 70^o$ a maximum force density of 800 Nm^{-3} has been deduced from a mass response of 25 g. The results were compared with the numerical calculations. Fig. 4 compares the calculated effective Lorentz force density along the HMM axis within the dummy and the Δm measurements at up- and downwards field translation at f = 300 Hz. Also here a good agreement between the results is obvious. As can be seen the Lorentz force F_L depends on the axial dummy position. At $\varphi = 70^o$ a plateau of $F_L = 600$ Nm^{-3} over a central region of ~40 mm could be achieved. Note, such a force density exceeds markedly the required one to counter-act the maximum buoyancy-driven flow force density F_b to be expected

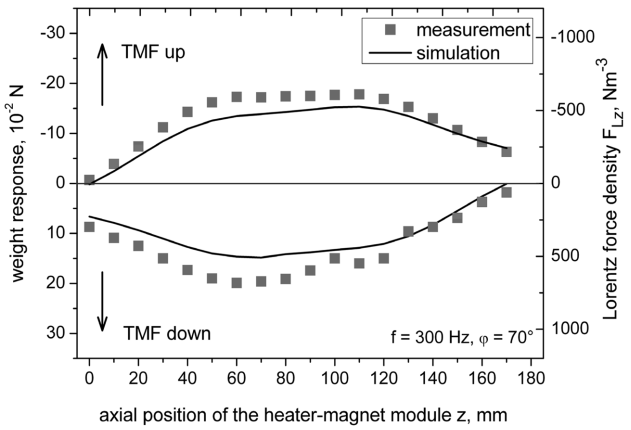

Fig. 4. Axial distribution of the measured and calculated mass response of the dummy within the heater-magnet module of the VGF equipment shown in Fig. 2 (see also ref. [19]) when an up- or downward TMF of I = 180 A per coil segment, f = 300 Hz and φ = 70° was induced. The right ordinate shows the deduced averaged Lorentz force density.

within the melt (see ch. 2). On the other side it demonstrates the strength and efficiency of the combined HMM very obviously.

6. Observation of Floating Particles

Visual observations of floating particles purposely placed on top of the melt are an excellent way to prove of which impact is the magnetic field on the melt flow. However, this is not possible in a VGF and conventional LEC arrangement due to the unobservability and hindrance of free particle movement by the encapsulating layer on the melt, respectively. Therefore, we used the VCz method without melt encapsulation [23] to visualize their unrestricted flow on the Ga-As melt surface by applying the standard viewing adjustment.

In contrast to the conventional mode without magnetic field, controllable melt flow patterns were obtained as function of the magnetic field parameters. We observed that the melt flow can be directed toward the crucible wall against the Marangoni convection driven forces. By just changing the direction of the TMF, the melt flow direction can be reversed. Flow vortices were obtained when the Lorentz force was increased over a critical value. These experiments have been very helpful to verify the reaction time of the melt flow patterns to changes of TMF parameters. In case of possible particles on the melt surface, their drift can be controlled very effective during the whole growth process. Fig. 5a shows such a VCz GaAs crystals grown under the influence of a TMF.

Fig. 5. GaAs (a, b) and Ge (c) single crystals grown by VCz (a), LEC (b) and VGF (c) under TMF generated in combined heater-magnet modules.

7. Growth Results

7.1. LEC of GaAs

For the first time, the feasibility of LEC growth within TMFs by applying HMM were tested. 3-in diameter [001]-oriented GaAs crystals were grown within an multi-coil AC-provided HMM design shown in Fig. 1b-c. Different TMFs were applied by varying frequency and phase shift in the ranges f = 50~400 Hz and φ = 5~90°, respectively.

In Fig. 5b, an as-grown LEC crystal is represented. Relatively good diameter stability has been obtained in case of high field frequencies of f = 300~400 Hz. On the other hand, at low frequency of f = 50 Hz the unfavorable concavity of the interface rim could be reduced most effectively. We found that the used HMM dampens temperature fluctuations under the growing crystal, especially, when higher TMF frequencies are used. Very weak and uniform residual striations have been revealed (Fig. 6) using microscopic etching by diluted Sirtl with light (DSL). The samples are taken from crystals grown at f = 300 and φ = 70° and were cut parallel to the growth axis. We assume that the residual striations are caused by the crucible-crystal rotation only.

Mean dislocation densities of ~10^4 cm^{-2} have been obtained. Minimum values of (4~5) × 10^3 cm^{-2} at half radius along the radial <100> - directions were observed in crystals grown at low TMF frequency.

Low residual impurity concentrations in the range of

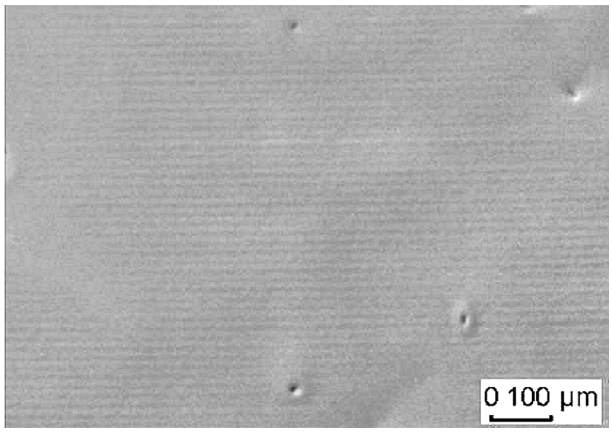

Fig. 6. Very waek and high-periodical residual striations in a longitudinal cut taken from an as-grown GaAs crystal obtained under TMF with f = 300 Hz and φ = 70°.

10^{13}~10^{14} cm^{-3} of metals have been measured by glow discharge mass spectrometry (GDMS). Surprisingly, markedly enhanced contents of oxygen and boron have been detected exceeding 10^{18} cm^{-3}. As a result, the substitutional carbon concentrations [C_{As}] measured by local vibrational mode (LVM) absorptions distinctly decreased below 10^{16} cm^{-3}. [C_{As}] is related to the high oxygen content according the activity contrariness of the chemical CO and O potentials in a LEC system [24]. At present, we assume that TMF-induced high-speed vortices under the boric oxide encapsulant [22] contribute essentially to the O and B release from it and their transport to the growing interface.

The as-grown crystals show semi-insulating behavior with specific electrical resistivities in the range of $\rho_e = (2\sim4) \times 10^8$ Ω cm, free carrier concentrations of $n = (3\sim6) \times 10^6$ cm^{-3} and electron mobilities of $\mu_n = 5000\sim6000$ cm^2/Vs measured by van der Pauw method at 300 K. The ρ_e values correlate with the carbon concentrations in the range of $C_{As} = (5\sim9) \times 10^{15}$ cm^{-3} as it is known from standard LEC crystals [24]. Finally, in comparison to standard as-grown LEC material relatively low $EL2^0$ concentrations in the range of $(0.5\sim1.2) \times 10^{16}$ cm^{-3} were ascertained.

7.2. VGF of Ge

As it is well known favourable flat or slightly convex melt-solid interface cannot be achieved under conventional VGF growth conditions, especially, in semiconducting materials [19]. To demonstrate the feasibility in travelling magnetic fields <111> - and <100> - oriented Ge single crystals with diameter of 110 mm and weight up to 6 kg were grown in a HMM VGF arrangement generating downward-directed Lorentz forces (Fig. 5c). More experimental details can be found elsewhere [7, 19].

For the investigation of the interface curvature by the striation technique the as-grown crystals were longitudinally cut along the <211> and <110> directions and then analysed by etching and lateral photo voltage scanning (LPS) [25]. The etch pit density (EPD) was determined on polished {111} and {100} planes by standard etchants and the physical parameters were ascertained by van der Pauw measurements at 300 K.

The striation-revealed interface morphology in Fig. 7a taken from a longitudinal cut of a Ge crystal grown under nearly optimum TMF conditions refers to flat and slightly convex interface shapes within the central region. A combined AC/DC programming of TMF and heating power according the numeric estimation was applied to consider the decreasing aspect ratio of the melt during the crystallization process. A very sensitive TMF impact on the melt-solid interface morphology without changing the heating conditions has been observed.

Fig. 7b~c represent striation images of the microscopic scale taken from crystals grown under different TMF conditions. When overcritical conditions with

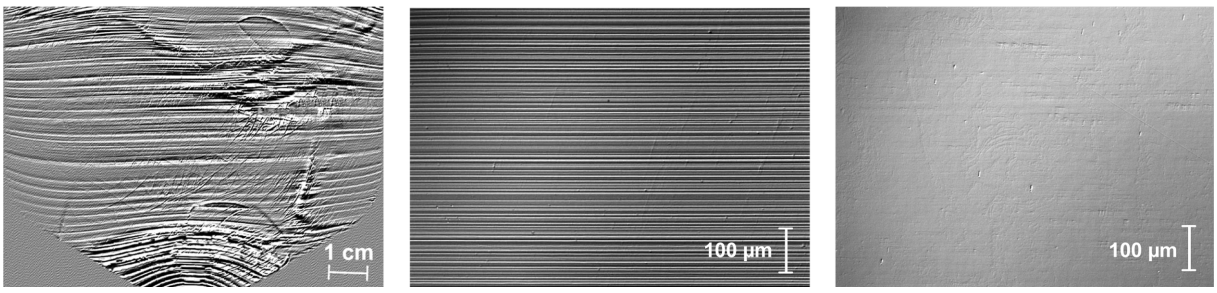

Fig. 7. a - LPS revealed interface shape of a Ge crystal grown under nearly optimum TMF contions. b, c - striation analysis on microscopic scale taken from longitudinal cuts of different as-grown 4-inch VGF Ge crystals obtained under overcritical TMF conditions (b) and under nearly optimized TMF parameters (c). Note, contrast variations in (a) represent carrier density differences due to the high characteristic LPS sensitivity [25].

$Ta_{TMF} \approx 10^8$ where chosen distinct striations were ascertained (b). They correlate very well with the numerically obtained fluctuation frequency of $f \approx 0.18$ Hz induced by reinforced TMF. It has been found that the striation intensity reduces and the interspace increases with lowering magnetic induction. Finally, when an optimized TMF was used nearly striation-free feature is observed (c). Therefore, our experimental results verify that convection-driven temperature fluctuations can be effectively damped by a well-adopted TMF. Comparable results have been reported by Lantzsch *et al.* [8] using, however, a more expensive TMF coil outside the growth chamber.

Etch pit densities (EPD) of $(0.6\sim3) \times 10^3$ cm^{-2} were found when optimum TMF conditions for ensuring a stationary flow regime and slightly convex interface were adjusted. In <100> - oriented crystals the centre was even free of dislocations. Such crystals show carrier concentrations $n_p = (0.9\sim2.8) \times 10^{15}$ cm^{-3} and mobilties $\mu_p = 2500\sim2800$ cm^{2}V^{-1}s^{-1}. An markedly improved radial parameter distributions homogeneity takes place when TMF is applied [19]. This is due to the flattening of the interface by a well selected downward TMF. From our first results we can conclude that an optimal adjusted TMF is of favorable influence on the structural and electrical qualities of as-grown VGF 4-inch Ge crystals.

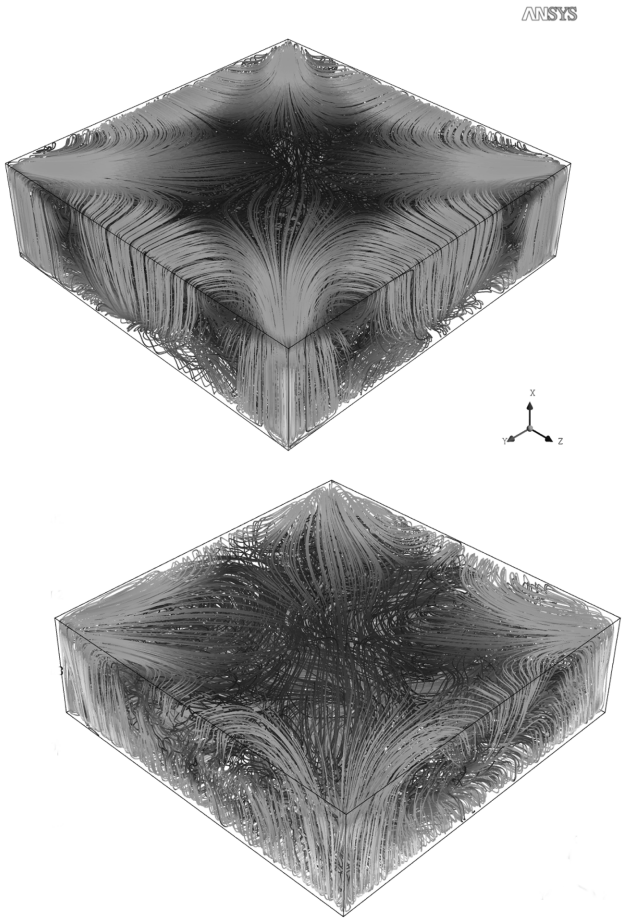

Fig. 8. Numeric simulation of the flow patterns in silicon melt within rectangular container without (a) and with TMF (b).

8. Conclusions and Outlook

First very hopeful results of GaAs and Ge crystals growth by LEC and VGF under TMFs generated together with heat in heater-magnet modules have been obtained within the framework of the KRIST*MAG*® project. Striation-free semi-insulating LEC GaAs crystals can be grown in a multi-coil HMM that allows to damp the harmful temperature fluctuations below the growing crystal. The EPD and electrical crystal properties show standard as-grown behaviour. Further experiments will be concentrated on the reduction of oxygen and boron contents by optimizing the TMF induced stream pattern.

High-quality VGF Ge single crystals were grown in a HMM simultaneously generating heat by DC and TMF by AC. Well adjusted AC/DC relation, low frequencies in the range of $f = 20\sim50$ Hz and magnetic field programming proved to be most suitable conditions to ensure a constant slightly convex crystallization front during the whole growth run. Striations are depressed by using undercritical TMF parameters. Low EPD, high carrier mobility and markedly improved radial homogeneity of electrical parameters were obtained in the as-grown crystals.

Meanwhile our attention is turned to applicability of TMFs also in production processes of silicon for photovoltaics. As a start the solidification of silicon in rectangular crucibles of dimension $70 \times 70 \times 20$ cm^3 is numerically investigated by fully 3D simulation using the commercial softwares Ansys Classic and Ansys CFX [26]. We found, that TMF is of significant influence on the flow structure. It can be used for both damp flow instabilities and mix the melt effectively. Fig. 8 shows the improvement of flow homogeneity when TMF is applied.

Acknowledgement

The authors are indebted to R.-P. Lange, M. Ziem, Dr. U. Juda, Th. Wurche, M. Imming, K. Banse, Dr. A. Lüdge, M. Pietsch, R. Menzel, Prof. R. Fornari (direc-

tor of IKZ), Dr. Ch. Lechner, Prof J. Sprekels (director of WIAS), Dr. H. Kasjanow, Prof. B. Nacke (director of ETP, Leibniz University of Hanover), and the teams of Steremat GmbH and Auteam GmbH for very fruitful cooperation.

The KRIST*MAG*® project was co-financed by the European Regional Developments Fund (EFRE), "Zukunfts-fonds" Berlin and "Zukunftsagentur" of the State Brandenburg.

References

[1] D.T.J. Hurle and R.W. Series, "The use of a magnetic field in melt growth" in: D.T.J. Hurle (ed.), Handbook of Crystal Growth, Vol. 2a (Elsevier, North-Holland 1994) p. 259.

[2] P. Dold and K.W. Benz, "Rotating magnetic fields: fluid flow and crystal growth applications", Prog. Cryst. Growth Charact. Mater. 38 (1999) 7.

[3] K. Kakimoto, "Modeling of fluid dynamics in the Czochralski growth of semiconductor crystals" in: G. Müller, J.-J. Metois, P. Rudolph (eds.), Crystal Growth - from Fundamentals to Technology (Elsevier, Amsterdam, 2004) p. 169.

[4] B.-C. Sim, I.-K. Lee, K.-H. Kim and H.-W. Lee, "Oxygen concentration in the Czochralski-grown crystal with cusp-magnetic field", J. Crystal Growth 275 (2005) 455.

[5] A. Moreno, B. Quiroz-Garcia, F. Yokaichiya, V. Stojanoff and P. Rudolph, "Protein crystal growth in gels and stationary magnetic fields", Cryst. Res. Technol. 42 (2007) 231.

[6] S. Yesilyurt, S. Motakef, R. Grugel and K. Mazuruk, "The effect of the traveling magnetic field (TMF) on the buoyancy-induced convection in the vertical Bridgman growth of semiconductors", J. Crystal Growth 263 (2004) 80.

[7] Ch. Frank-Rotsch, D. Jockel, M. Ziem and P. Rudolph, "Numerical optimization of the interface shape at the VGF growth of semiconductor crystals in a traveling magnetic field", J. Crystal Growth 310 (2008) 1505.

[8] R. Lantzsch, I. Grants, O. Pätzold, M. Stelter and G. Gerbeth, "Vertical gradient freeze growth with external magnetic fields", J. Crystal Growth 310 (2008) 1518.

[9] Th. Wetzel, "Die Schmelzströmung im Si-Czochralski-Prozeβ unter dem Einfluβ elektromagnetischer Felder", Fortschritt-Berichte VDI, Reihe 9, Nr. 328 (2001) 1.

[10] E. Tomzig, J. Virbulis, W.v. Ammon, Y. Gelfgat and L. Gorbunov, "Application of dynamic and combined magnetic fields in the 300 mm silicon single-crystal growth", Mat. Sci. in Semicond. Processing 5 (2003) 347.

[11] A. Krauze, A. Muiznieks, A. Mühlbauer, Th. Wezel, L. Gorbunov, A. Pedchenko and J. Virbulis, "Numerical 2D modelling of turbulent melt flow in CZ system with dynamic magnetic fields", J. Crystal Growth 266 (2004) 40.

[12] O. Klein, P.-E. Druet, Ch. Lechner *et al.*, "Numerical simulation of Czochralski crystal growth under the influence of a traveling magnetic field generated by internal heater-magnet module (HMM)", J. Crystal Growth 310 (2008) 1523.

[13] P. Rudolph, "Travelling magnetic fields applied to bulk crystal growth from the melt: the step from basic research to industrial scale", J. Crystal Growth 310 (2008) 1298.

[14] P. Rudolph, Ch. Frank-Rotsch, F.-M. Kiessling *et al.*, "Crystal growth in heater-magnet modules - from concept to use", in: Proc. Int. Scientific Colloquium Modelling for Electromagnetic Processing (MEP 08), October 27-29, 2008 in Hanover, p. 79.

[15] P. Rudolph, M. Ziem and P. Lange, Patent DE 10 2007 020 239, WO 2007/122231.

[16] Ch. Frank-Rotsch, P. Rudolph, O. Klein, P. Lange and B. Nacke, Patent DE 10 2007 028 548, WO 2008/155137.

[17] P. Lange, D. Jockel, M. Ziem *et al.*, Patent DE 10 2007 028 547, WO 2008/155138.

[18] P. Schwesig, M. Hainke, J. Friedrich and G. Mueller, "Comparative numerical study of the effects of rotating and travelling magnetic fields on the interface shape and thermal stress in the VGF growth of InP crystals", J. Crystal Growth 266 (2004) 224.

[19] Ch. Frank-Rotsch and P. Rudolph, "Vertical gradient freeze of 4 inch Ge crystals in a heater-magnet module", J. Crystal Growth 311 (2009) 2294.

[20] Ch. Frank-Rotsch, P. Rudolph, O. Klein *et al.*, Patent DE 10 2007 028 548, WO 2008/155137.

[21] H. Kasjanow, B. Nacke, St. Eichler *et al.*, "3D numerical modeling of asymmetry effects of a heater-magnet module for VGF and LEC growth under traveling magnetic fields", J. Crystal Growth 310 (2008) 1540.

[22] O. Klein, Ch. Lechner, P.-E. Druet *et al.*, "Numerical simulations of the influence of a traveling magnetic field, generated by an internal heater magnet module, on Czochralski crystal growth", Proc. Intern. Sci. Colloquium "Modelling for Electromagnetic Processing" (MEP 08), October 27-29, 2008 in Hanover, pp. 91.

[23] P. Rudolph and F.-M. Kiessling, "Growth and characterization of GaAs crystals produced by the VCz method without boric oxide encapsulation", J. Crystal Growth 292 (2006) 532.

[24] M. Jurisch, F. Börner, Th. Bünger *et al.*, "LEC- and VGF-growth of SI GaAs single crystals - recent developments and current issues", J. Crystal Growth 275 (2005) 283.

[25] N.V. Abrosimov, A. Lüdge, H. Riemann and W. Schröder, "Lateral photovoltage scanning (LPS) method for the visualization of the solid-liquid interface of $Si_{1-x}Ge_x$ single crystals", J. Crystal Growth 237-239 (2002) 356.

[26] N. Dropka, W. Miller, R. Menzel and U. Rehse, "Numerical study on transport phenomena in a directional solidification process in the presence of travelling magnetic fields" (in press), doi:10.1016/j.jcrysgro.2009.09.016.